

Time-of-day immunochemotherapy in nonsmall cell lung cancer: a randomized phase 3 trial

Received: 22 July 2025

Accepted: 11 December 2025

Published online: 02 February 2026

 Check for updates

A list of authors and their affiliations appears at the end of the paper

Retrospective studies suggest that early time-of-day (ToD) infusions of immunochemotherapy may improve efficacy. However, prospective randomized controlled trials are needed to validate it. In this randomized phase 3 LungTIME-C01 trial, 210 patients with treatment naive stage IIIc–IV nonsmall cell lung cancer (NSCLC) lacking driver mutations were randomly assigned in a 1:1 ratio to either an early or late ToD group, defined by the administration of the first four cycles of an anti-PD-1 agent before or after 15:00 h. The primary endpoint was progression-free survival (PFS), while secondary endpoints included overall survival (OS) and objective response rate (ORR). After a median follow-up of 28.7 months, the median PFS was 11.3 months (95% confidence interval (CI) = 9.2–13.4) in the early ToD group and 5.7 months (95% CI = 5.2–6.2) in the late ToD group, corresponding to a hazard ratio (HR) for earlier disease progression of 0.40 (95% CI = 0.29–0.55; $P < 0.001$). The median OS was 28.0 months (95% CI = not estimable (NE)–NE) in the early ToD group and 16.8 months (95% CI = 13.7–19.9) in the late ToD group, corresponding to an HR of an earlier death of 0.42 (95% CI = 0.29–0.60; $P < 0.001$). Treatment-related adverse events were consistent with the established safety profile, with no new safety signals observed. No significant differences in immune-related adverse events were observed between the two groups. Over the first four cycles, morning circulating CD8⁺ T cells increased in the early ToD group, whereas they declined in the late ToD group ($P < 0.001$). Furthermore, the ratio of activated (CD38⁺ HLA-DR⁺) versus exhausted (TIM-3⁺PD-1⁺) CD8⁺ T cells was higher in the early ToD group ($P < 0.001$) compared with the late ToD group ($P < 0.001$). In summary, our study indicates that early ToD immunochemotherapy substantially improves PFS and OS and is associated with enhanced antitumor CD8⁺ T cell characteristics compared with late ToD treatment. ClinicalTrials.gov registration: NCT05549037.

 e-mail: tony@clo.cuhk.edu.hk; christoph.scheiermann@unige.ch; francis.levi@universite-paris-saclay.fr; yangnong0217@163.com; zhangyongchang@csu.edu.cn

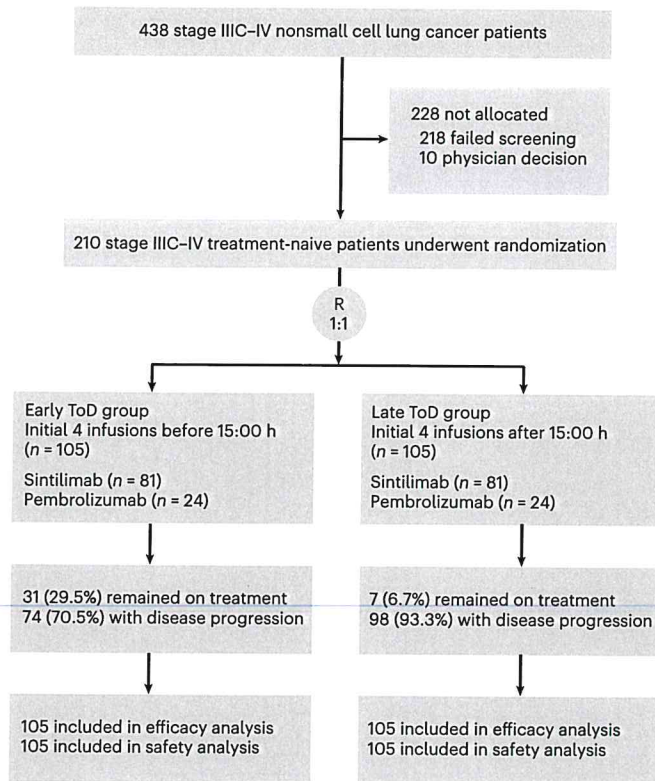


Fig. 1 | Flowchart of the present study. From September 2022 to May 2024, 210 patients were enrolled. Data cutoff time was 31 August 2025.

Immune checkpoint inhibitors (ICIs) have improved treatment outcomes for patients with advanced non-small cell lung cancer (NSCLC)^{1–4}. However, a substantial fraction of patients (~10% to 15%) neither respond to ICI therapy nor show long-term benefits⁵. Objective response rates (ORRs) remain below 50% and only a fraction may achieve long-term survival⁶.

Circadian rhythms exert a substantial influence on the distribution and function of immune cells. These oscillations have emerged as key regulators of immune responses and may, therefore, impact the efficacy of immunotherapy^{7–11}. More than 20 retrospective studies have demonstrated improvement in the efficacy of ICIs given at early rather than late times of the day (ToD)^{12–17}. In addition, a meta-analysis of 13 retrospective studies demonstrated that OS and PFS were nearly doubled among patients receiving single-agent or combined ICIs administered at early ToD¹⁸. The impact of the infusion ToD was consistent across multiple tumor types, including renal cell carcinoma, malignant melanoma and others^{18,19}.

A simple adjustment in the timing of immunotherapy infusions may enhance therapeutic efficacy¹⁹. However, findings from retrospective studies are susceptible to confounding factors, including imbalances in patient characteristics, programmed death ligand 1 (PD-L1) status and dose intensity of ICI infusions²⁰. Therefore, a prospective randomized controlled trial is required to validate this retrospective observation.

Here we report results of a phase 3 randomized controlled trial (LungTIME-C01) comparing early versus late ToD infusion of first-line chemo-immunotherapy in patients with advanced NSCLC.

Results

Patient characteristics and treatment regimes

A total of 438 patients with stage IIIC–IV NSCLC lacking sensitizing *EGFR/ALK/ROS1* alterations and eligible for first-line chemo-immunotherapy were screened for eligibility at Hunan Cancer

Hospital between 23 September 2022 and 21 May 2024 (Fig. 1). Reasons for screening failure included active brain metastases ($n = 7$), concurrent hormonal therapy ($n = 3$), active tuberculosis ($n = 2$), hepatitis B infection ($n = 2$), refusal of pembrolizumab or sintilimab ($n = 97$), use of traditional Chinese medicine ($n = 23$) and refusal to accept treatment timing stipulations ($n = 84$). A total of 210 patients were randomized to the early ToD group ($n = 105$) or to the late ToD group ($n = 105$). Baseline demographics and disease characteristics were well balanced between the two groups (Table 1). Among the 210 randomized patients, 190 (90.5%) were male and 171 (81.4%) had a history of smoking. PD-L1 tumor proportion score (TPS) was available for 196 patients (93.3%) and distributed as follows: <1% for 88 patients (41.9%), 1–49% for 60 patients (28.6%) and $\geq 50\%$ for 48 patients (22.9%). The majority of patients ($n = 162$, 77.1%) received sintilimab, whilst 48 patients (22.9%) received pembrolizumab. A total of 58 patients (27.6%) had baseline lactate dehydrogenase levels >1 upper limit of normal. Lung Immune Prognostic Index (LIPI) scores were distributed as follows: low risk in 121 patients (57.6%), medium risk in 72 patients (34.3%) and high risk in 17 patients (8.1%). All patients received their first four cycles of immunotherapy within the assigned protocol-defined ToD window (before or after 15:00 h), unless treatment was discontinued due to early progression. The median clock hour times to start ICI infusion in the early and late ToD group were 10:55 h (range = 7:34–14:00 h; China Standard Time, CST) and 15:57 h (range = 15:00–20:39 h), respectively (Extended Data Fig. 1 and Extended Data Table 1). Four or more ICI-containing treatment courses were administered to 98.1% of patients in the early ToD group and 96.2% of the patients in the late ToD group. The majority of patients assigned to the early ToD group continued to receive infusions predominantly before 15:00 h, while those in the late ToD group predominantly received them after 15:00 h, despite the lack of any protocol stipulation for ToD treatments after the fourth cycle. The median infusion time of the fifth, sixth and seventh cycles occurred before 15:00 h for 77.0% of the patients ($n = 67/87$) in the early ToD group, compared to 38.5% of the patients in the late ToD group ($n = 30/78$; $P < 0.001$).

The data cutoff date was 31 August 2025, at which time the median follow-up duration was 28.7 months (range = 1.4–35.2). The median duration of immunotherapy was 10.4 months (range = 1 day to 33.4 months, interquartile range = 4.9–20.5 months) in the early ToD group and 4.5 months (range = 1 day to 34.2 months, interquartile range = 2.8–8.3 months) in the late ToD group. Treatment withdrawal due to progressive disease occurred in 172 events (81.9%), as confirmed by the Blinded Independent Review Committee (BIRC; Extended Data Table 1). At the cutoff date, 31 patients (29.5%) in the early ToD group and 7 patients (6.7%) in the late ToD group remained on treatment (Fig. 1).

Efficacy

The median PFS was 11.3 months (95% confidence interval (CI) = 9.2–13.4) for the early ToD group and 5.7 months (95% CI = 5.2–6.2) for the late ToD group. The HR of an earlier progression in the early ToD group was 0.40 (95% CI = 0.29–0.55, $P < 0.001$; Fig. 2a). The 1-year PFS rates were 47.6% (95% CI = 39.0–58.2%) and 19.0% (95% CI = 12.8–28.3%) for the early and late ToD group, respectively. HRs for earlier disease progression were <0.55 in all subgroups, except for the small subset of 16 patients with liver metastases (Fig. 2b).

At the data cutoff, 126 survival events (60.0%) had occurred. Median OS was 28.0 months (95% CI = NE–NE) in the early ToD group compared to 16.8 months (95% CI = 13.7–19.9) in the late ToD group, with an HR of 0.42 (95% CI = 0.29–0.60, $P < 0.001$; Fig. 3a). The HRs for earlier death remained consistently below 0.63 across all subgroups (Fig. 3b).

Univariate or multivariate Cox regression analyses were performed on age, sex, smoking history, Eastern Cooperative Oncology Group Performance Status, histology, brain metastases, liver

Table 1 | Baseline characteristics of patient

Characteristics	Early ToD group (n=105)	Late ToD group (n=105)	P value
Age (year, median, range)	61 (33–80)	60 (34–77)	0.53
Sex (n, %)			
Male	95 (90.5)	95 (90.5)	1.000
Female	10 (9.5)	10 (9.5)	
Smoking history (n, %)			
Smoker	84 (80.0)	87 (82.9)	0.590
Never smoked	21 (20.0)	18 (17.1)	
ECOG PS (n, %)			
0	38 (36.2)	32 (30.5)	0.380
1	67 (63.8)	73 (69.5)	
Histology (n, %)			
Squamous	60 (57.1)	56 (53.3)	0.580
Adenocarcinoma	45 (42.9)	49 (46.7)	
Stage (n, %)			
IIIc	24 (22.9)	17 (16.2)	0.120
IV	81 (77.1)	88 (83.8)	
Brain metastasis (n, %)			
Yes	13 (12.4)	16 (14.3)	0.550
No	92 (86.7)	89 (84.8)	
Liver metastasis (n, %)			
Yes	6 (5.7)	10 (9.5)	0.300
No	99 (94.3)	95 (90.5)	
PD-L1 TPS (n, %)			
<1%	41 (39.0%)	47 (44.8%)	0.862
1–49%	31 (29.5%)	29 (27.5%)	
≥50%	26 (24.8%)	22 (21.0%)	
Unknown	7 (6.7%)	7 (6.7%)	
ICIs (n, %)			
Sintilimab	81 (77.1%)	81 (77.1%)	1.000
Pembrolizumab	24 (22.9%)	24 (22.9%)	
Tumor burden (n, %)			
≥80mm	56 (53.3)	43 (41.0)	0.097
<80mm	49 (46.7)	62 (59.0)	
LDH (n, %)			
≤1 ULN	79 (75.2)	73 (69.5)	0.440
>1 ULN	26 (24.8)	32 (30.5)	
LIPI score (n, %)			
Low risk	63 (60.0)	58 (55.2)	0.673
Medium risk	35 (33.3)	37 (35.3)	
High risk	7 (6.7)	10 (9.5)	

Immunochemotherapy administration started before 15:00h in the early ToD group and at or after 15:00h in the late ToD group. ECOG PS, Eastern Cooperative Oncology Group Performance Status; LDH, lactate dehydrogenase; ULN, upper limit of normal.

metastases, PD-L1 TPS, ICI agent, LIPI score and ToD. Among these, only ToD and PD-L1 TPS were substantial predictors of both PFS and OS (Extended Data Fig. 2a,b).

Objective responses differed between the two treatment groups. ORRs were 69.5% (95% CI = 60.6–78.5%) for the early ToD group

and 56.2% (95% CI = 46.5–65.8%) for the late ToD group ($P = 0.046$; Extended Data Fig. 3).

Adverse events

Hematologic adverse events, including both any grade and grade 3–4 (leukopenia, anemia and thrombocytopenia), were the most common (Extended Data Tables 2 and 3). Notably, there were no adverse events leading to death or treatment discontinuation in either group. Hematologic toxicities of any grade were more common in the early ToD group, with leukopenia (any grade) occurring in 44.8% and 28.6% of patients in the early and late ToD group, respectively ($P = 0.015$). However, no significant differences were observed in other toxicities (any grade; Extended Data Table 2). Immune-related adverse events were observed in both groups, with hypothyroidism and rash being the most common (any grade; Extended Data Table 3). There were no statistically significant differences found in the incidence of immune-related adverse events between the two groups (Extended Data Table 3).

Peripheral blood lymphocyte subsets

Flow cytometric analyses of CD3⁺, CD4⁺, CD8⁺ T cells, B cells and NK cells were performed on 61 patients in the early ToD group and 44 patients in the late ToD group at three time points (baseline, after cycle 2 and after cycle 4 of immunochemotherapy). Among patients included in the flow cytometry analysis, no significant differences in baseline demographics or disease characteristics were observed between the early ToD and late ToD groups (Extended Data Table 4). We detected a substantial increase in the percentage of circulating CD3⁺ T cells ($P < 0.001$; Fig. 4a and Extended Data Fig. 4a) and circulating CD8⁺ T cells ($P < 0.001$; Fig. 4b and Extended Data Fig. 4b) after cycle 2 and 4 in the early ToD group. In contrast, the percentage of circulating CD3⁺ T cells and CD8⁺ T cells decreased after cycle 4 in the late ToD group (Fig. 4a,b and Extended Data Fig. 4a,b). In the late ToD group, there was an upward trend in the percentages of circulating CD4⁺ T cells, B cells and NK cells, while these populations remained stable in the early ToD group. However, the differences among groups over time were not statistically significant ($P = 0.088$ for CD4⁺ T cells, $P = 0.098$ for B cells and $P = 0.071$ for NK cells; Extended Data Fig. 4c–h). Notably, the CD8⁺/CD4⁺ T cell ratio increased in patients receiving early ToD immunochemotherapy, whereas it decreased in the late ToD group ($P < 0.001$; Fig. 4c and Extended Data Fig. 4i). Additional exploratory analyses were performed to evaluate the extent of CD8⁺ T cell activation (CD38⁺ HLA-DR⁺) and exhaustion (TIM-3⁺PD-1⁺) from cryopreserved peripheral blood mononuclear cells obtained from a small cohort of trial patients (early ToD, $n = 14$; late ToD, $n = 25$; Extended Data Fig. 5a, gating strategy). The percentage of CD38⁺ HLA-DR⁺ CD8⁺ T cells increased in both groups, with no significant difference observed between the early and late ToD groups ($P = 0.238$; Extended Data Fig. 5b,c). In contrast, the percentage of TIM-3⁺PD-1⁺ CD8⁺ T cells increased in the late ToD group but decreased in the early ToD group ($P = 0.014$; Fig. 4d and Extended Data Fig. 5d). As a result, following treatment, the early ToD group exhibited a markedly elevated ratio of CD38⁺ HLA-DR⁺ CD8⁺ T cells to TIM-3⁺PD-1⁺ CD8⁺ T cells compared to the late ToD group ($P < 0.001$; Fig. 4e and Extended Data Fig. 5e). Our exploratory analysis suggests that these treatment-induced changes in the peripheral blood composition and phenotype of lymphocyte subsets may be associated with the ToD of administration, and in turn, may also be linked to the efficacy of immunochemotherapy.

Discussion

This prospective, randomized controlled trial confirms the influence of ToD of immunochemotherapy infusion on treatment efficacy in patients with advanced NSCLC. Early ToD infusions of sintilimab or pembrolizumab in combination with chemotherapy resulted in statistically significant improvements in PFS, OS and ORR compared with late ToD infusions. These results are consistent with the findings from

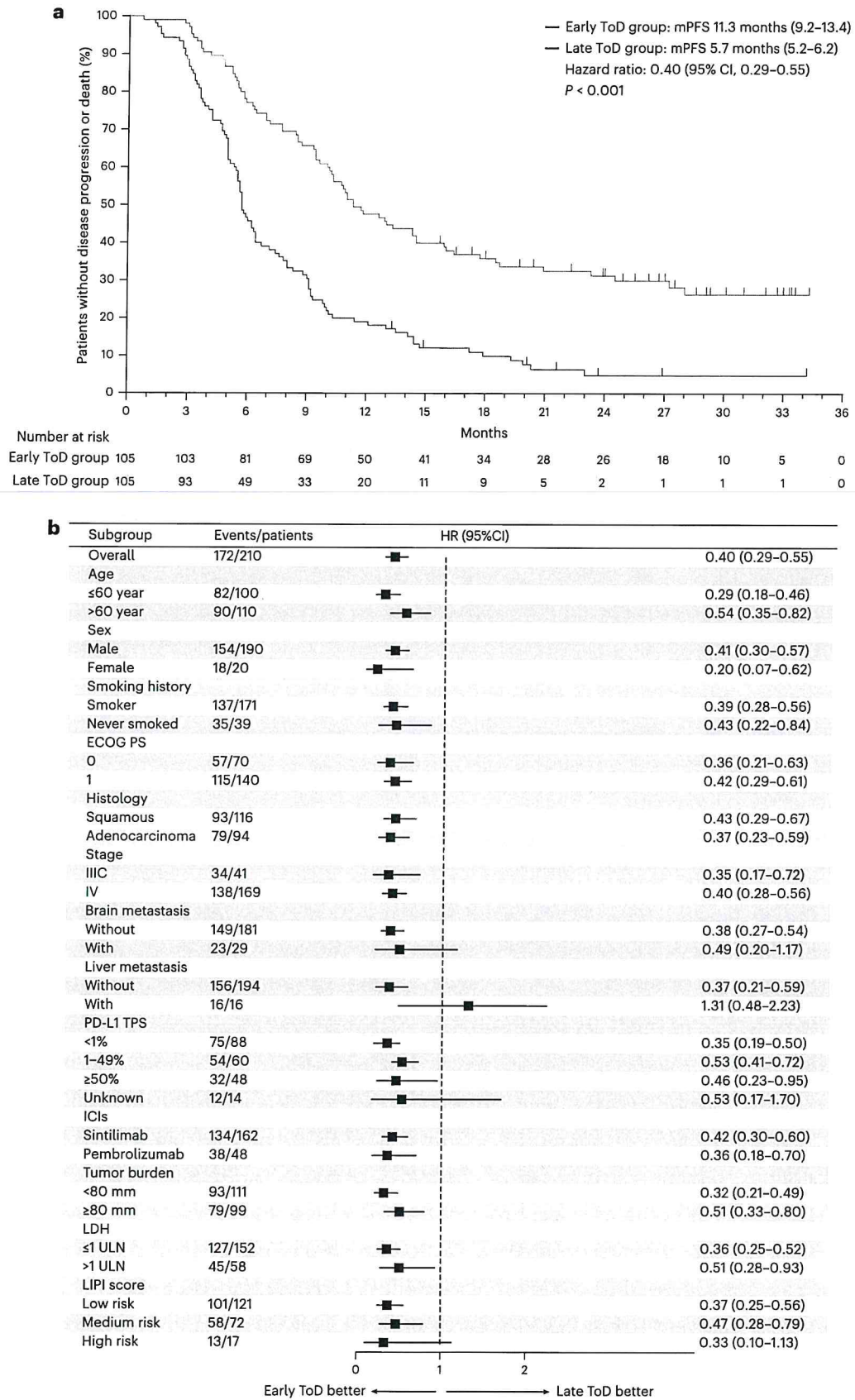


Fig. 2 | PFS of early vs late ToD treatment group. a, Kaplan–Meier curves for PFS in both groups ($n = 210$). Colors indicate group allocation: blue, early ToD; red, late ToD. A two-sided log-rank test was used to calculate P values. Cox proportional hazards regression was used to estimate HR and 95% CI. **b**, Forest

plot of the HR and 95% CIs of an earlier progression or death according to main patient characteristics ($n = 210$). Cox proportional hazards regression was used to estimate HR and 95% CI. Data are presented as HR (points) with 95% CIs (horizontal lines). mPFS, median progression-free survival; LDH, lactate dehydrogenase.

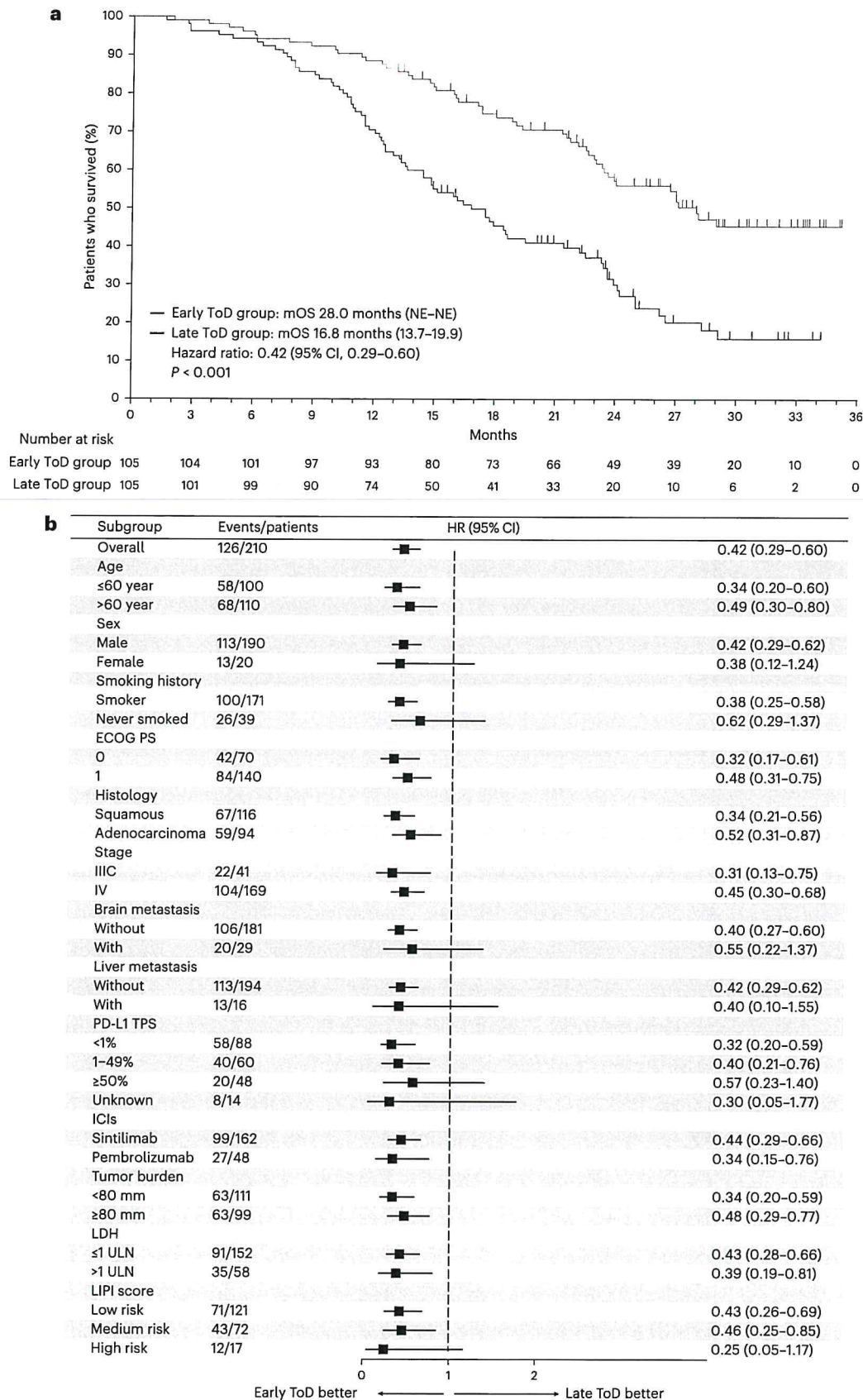


Fig. 3 | OS of early vs late ToD treatment groups. a, Kaplan–Meier curves for OS in both cohorts ($n = 210$). A two-sided log-rank test was used to calculate P values. Treatment cohorts are distinguished by color scheme: early ToD is depicted in blue, whereas late ToD is depicted in red. Cox proportional hazards regression was used

to estimate HR and 95% CI. **b**, Forest plot of the HR and 95% CI of an earlier death according to main patient characteristics ($n = 210$). Cox proportional hazards regression was used to estimate HR and 95% CI. Data are presented as HR (points) with 95% CIs (horizontal lines). NE, not estimable; mOS, median overall survival.

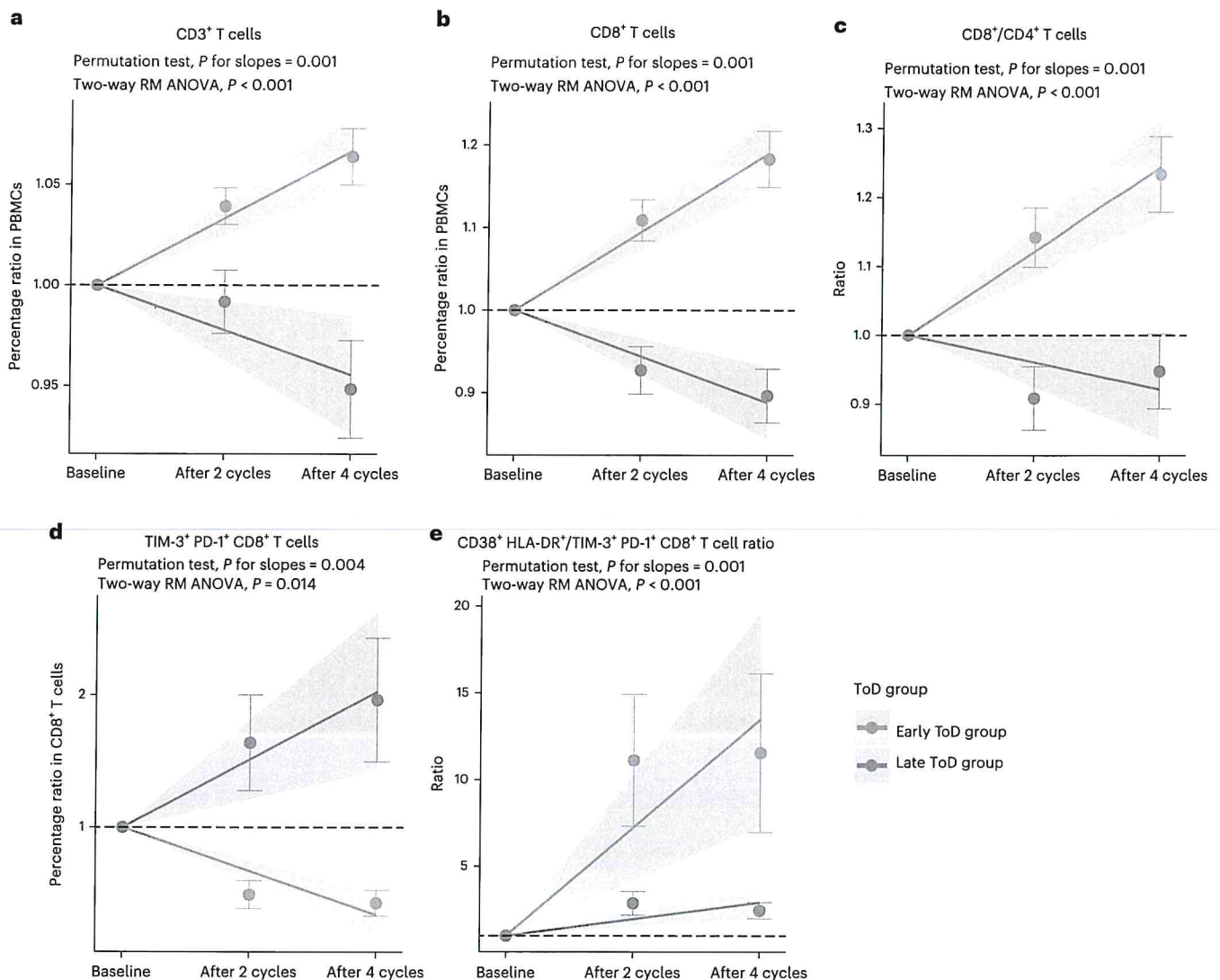


Fig. 4 | Changes in peripheral blood lymphocytes. Patient data are expressed relative to individual baseline levels after two cycles (before the third cycle) and four cycles (before the fifth cycle) of immunochemotherapy. **a–e**, Linear regressions (solid lines) and their 95% CIs (shaded areas) showed the trend of changes of CD3⁺ T cell proportion (**a**), CD8⁺ T cell proportion (**b**), the CD8⁺/CD4⁺ T cell ratio (**c**), TIM-3⁺ PD-1⁺ CD8⁺ T cell proportion (**d**) and the CD38⁺ HLA-DR⁺/TIM-3⁺ PD-1⁺ CD8⁺ T cell ratio (**e**) over time in early ToD group and late ToD group. Data are presented as mean \pm s.e.m. Dotted horizontal lines indicate the normalized baseline (ratio = 1.0). P values were determined using a permutation test (two-sided) and two-way repeated-measures ANOVA

(two-sided), without adjustment for multiple comparisons. Flow cytometric analyses of CD3⁺, CD4⁺ and CD8⁺ T cells were performed on paired blood samples collected at baseline, after two cycles and after four cycles from 61 patients in the early ToD group and 44 patients in the late ToD group ($n = 105$ total patients; $n = 315$ total samples). CD38⁺ HLA-DR⁺ CD8⁺ T cells and TIM-3⁺ PD-1⁺ CD8⁺ T cells were assessed in paired cryopreserved PBMCs collected at baseline, after two cycles and after four cycles from 14 patients in the early ToD group and 25 patients in the late ToD group ($n = 39$ total patients; $n = 117$ total samples). Two-way RM ANOVA, two-way repeated measures analysis of variance; PBMCs, peripheral blood mononuclear cells.

multiple retrospective studies^{18–21}. Given that a substantial proportion of patients in the early ToD group remain on active treatment in the current trial, additional follow-up is necessary to evaluate long-term survival outcomes. The subgroup analyses indicated that treatment infusions at early ToD yielded comparable benefits regardless of the specific anti-PD-1 agent used or patient baseline characteristics, suggesting that the survival advantage of early administration may be consistent across different treatment settings and patient subgroups. We observed substantially improved PFS in the early ToD group across all PD-L1 subgroups (<1%, 1–49% and \geq 50%) and improved OS in patients with PD-L1 <1% and 1–49%. These findings have important implications for the routine clinical use of immunochemotherapy, offering a simple and cost-neutral strategy that can be readily implemented without imposing additional financial burden on the healthcare system.

Although no specific infusion timing was mandated for patients beyond the initial four cycles, our data show that the subsequent three treatment cycles were administered to most patients within their originally assigned infusion time window. Thus, the observed effects of ToD may not be attributable solely to the ToD of the initial four cycles or to the ToD of immunotherapy alone, given its combination with chemotherapy. Nonetheless, this does not alter our conclusion that earlier ToD infusion of the standard immunochemotherapy protocol for NSCLC is associated with improved clinical outcomes.

Most published clinical trials involving ICIs have overlooked the potential influence of circadian rhythms. The lack of documentation or consideration of infusion ToD in trial designs may unintentionally affect study outcomes. Our findings suggest that failing to account for this factor could introduce confounding bias. For example, three

randomized phase 3 studies evaluated the role of adjuvant single-agent ICI in patients with resectable early-stage NSCLC, namely IMpower 010, KEYNOTE-091 and BR.31 (ref. 22–24). While two studies reported positive outcomes overall, it remained unclear why the KEYNOTE-091 trial failed to show a survival benefit in the high PD-L1 expression subgroup. BR.31, on the other hand, showed no improvement in either event-free survival or OS. Multiple confounding variables could explain these discrepancies and the timing of ICI administration should now be considered as one of the relevant factors. Large-scale real-world data analyses also reported better treatment outcomes with early ToD administration of immunochemotherapy²⁵. Our prospective randomized phase 3 trial adds further critical support to current knowledge, showing substantial improvements in PFS and OS with early ToD ICI administration. These findings underscore the importance of recording infusion times and considering ToD as a stratification factor in the design of future immunotherapy trials.

Immunophenotyping of peripheral blood demonstrated that early ToD infusions were associated with increased levels of circulating CD8⁺ T cells and a higher ratio of activated (CD38⁺ HLA-DR⁺) to exhausted (TIM-3⁺PD-1⁺) CD8⁺ T cells. These shifts in T cell subpopulations likely reflect increased cytotoxic activity and may partly explain the improved clinical efficacy observed in the early ToD group. Previous studies have also associated higher peripheral CD8⁺ T cell counts with improved tumor responses to ICIs^{26,27}. Although ICIs were traditionally believed to restore pre-existing but suppressed antitumor T cell responses, recent evidence indicates that they may also initiate de novo responses by priming circulating peripheral T cells, thus broadening the effective antitumor repertoire^{28,29}. Additional data, such as T cell proliferation measured by CD8⁺ Ki67⁺ and TCR repertoire, could further support this conclusion. However, as CD8⁺ T cell subsets were analyzed retrospectively on cryopreserved samples, the available sample size was limited and prolonged storage may have introduced bias. Further studies are warranted to confirm these findings. Moreover, the observed changes in immune subsets are known indicators of a favorable response to immunotherapy³⁰. Given the superior outcomes observed in the early ToD group, it remains challenging to determine whether these cellular effects are directly attributable to the timing of infusion or instead reflect a consequence of the improved clinical response. A study in ref. 31 demonstrated a change in both the quantity and the quality of tumor-infiltrating CD8⁺ T cells according to circadian rhythms and have shown their substantial impact on immunotherapy efficacy in both mouse and human cancer models. The relationship between blood-based immune cell status and tumor-infiltrating lymphocyte status remains unclear. While our data show obvious changes in peripheral immune profiles, the absence of paired post-treatment tumor biopsies prevents us from directly assessing differences in intratumoral immune responses between both ToD groups. Preclinical models suggest that increases in circulating CD8⁺ T cells can influence local immune activity³¹; however, further research is needed to confirm this effect in patients. Additionally, ToD-dependent leukocyte profiles are predictive for OS improvement in patients with advanced melanoma receiving anti-PD-1 therapy^{32,33}. Future investigations incorporating paired blood and tumor tissue samples will be essential to elucidate the relationship between peripheral and intratumoral immune responses and to more clearly define the mechanisms underlying the ToD-dependent efficacy of immunotherapy.

This single-center study was conducted in China and the findings may differ from those observed in Western populations, highlighting the need for further international multicenter studies to prospectively evaluate and extend the ToD-related findings across diverse populations, as suggested by multiple retrospective studies conducted across three continents. Although statistically significant differences in OS were observed between the two groups at the time of this analysis, the OS data have not yet matured. We will continue survival follow-up and report mature survival data upon reaching 65% of events. While our

lymphocyte subset data and existing evidence suggest that ToD effects may involve circadian modulation of immune cell infiltration and function, the underlying mechanisms remain incompletely understood in patients. These effects likely arise from complex interactions between immunological responses and drug pharmacokinetics, highlighting the need for further dedicated mechanistic studies.

In conclusion, infusion of immunochemotherapy at early ToD improves PFS and OS in patients with advanced NSCLC. Future clinical trials of immunotherapy should, at a minimum, document infusion time and may also consider incorporating infusion time as a stratification factor.

Online content

Any methods, additional references, Nature Portfolio reporting summaries, source data, extended data, supplementary information, acknowledgements, peer review information, details of author contributions and competing interests; and statements of data and code availability are available at <https://doi.org/10.1038/s41591-025-04181-w>.

References

- Benjamin, D. J. et al. The role of chemotherapy plus immune checkpoint inhibitors in oncogenic-driven NSCLC: a University of California lung cancer consortium retrospective study. *JTO Clin. Res. Rep.* **3**, 100427 (2022).
- Reck, M., Remon, J. & Hellmann, M. D. First-line immunotherapy for non-small-cell lung cancer. *J. Clin. Oncol.* **40**, 586–597 (2022).
- Martinez, P., Peters, S., Stammers, T. & Soria, J. C. Immunotherapy for the first-line treatment of patients with metastatic non-small cell lung cancer. *Clin. Cancer Res.* **25**, 2691–2698 (2019).
- Reck, M. et al. Five-year outcomes with pembrolizumab versus chemotherapy for metastatic non-small-cell lung cancer with PD-L1 tumor proportion score \geq 50. *J. Clin. Oncol.* **39**, 2339–2349 (2021).
- Huang, M. Y., Jiang, X. M., Wang, B. L., Sun, Y. & Lu, J. J. Combination therapy with PD-1/PD-L1 blockade in non-small cell lung cancer: strategies and mechanisms. *Pharmacol. Ther.* **219**, 107694 (2021).
- Meyer, M. L. et al. New promises and challenges in the treatment of advanced non-small-cell lung cancer. *Lancet* **404**, 803–822 (2024).
- Kisamore, C. O., Elliott, B. D., DeVries, A. C., Nelson, R. J. & Walker, W. H. II Chronotherapeutics for solid tumors. *Pharmaceutics* **15**, 2023 (2023).
- Cermakian, N. & Labrecque, N. Regulation of cytotoxic CD8⁺ T cells by the circadian clock. *J. Immunol.* **210**, 12–18 (2023).
- Amiama-Roig, A., Verdugo-Sivianes, E. M., Carnero, A. & Blanco, J. R. Chronotherapy: circadian rhythms and their influence in cancer therapy. *Cancers (Basel)* **14**, 5071 (2022).
- Ince, L. M. et al. Influence of circadian clocks on adaptive immunity and vaccination responses. *Nat. Commun.* **14**, 476 (2023).
- Wang, C. L., Zhang, X. & Dang, C. V. Clocking cancer immunotherapy responses. *Cancer Res.* **84**, 2756–2758 (2024).
- Qian, D. C. et al. Effect of immunotherapy time-of-day infusion on overall survival among patients with advanced melanoma in the USA (MEMOIR): a propensity score-matched analysis of a single-centre, longitudinal study. *Lancet Oncol.* **22**, 1777–1786 (2021).
- Patel, J. S. et al. Impact of immunotherapy time-of-day infusion on survival and immunologic correlates in patients with metastatic renal cell carcinoma: a multicenter cohort analysis. *J. Immunother. Cancer* **12**, e008011 (2024).
- Ruiz-Torres, D. A. et al. Immunotherapy time of infusion impacts survival in head and neck cancer: a propensity score matched analysis. *Oral Oncol.* **151**, 106761 (2024).

15. Nomura, M. et al. Timing of the infusion of nivolumab for patients with recurrent or metastatic squamous cell carcinoma of the esophagus influences its efficacy. *Esophagus* **20**, 722–731 (2023).
16. Hirata, T. et al. Brief report: clinical outcomes by infusion timing of immune checkpoint inhibitors in patients with locally advanced NSCLC. *JTO Clin. Res. Rep.* **5**, 100659 (2024).
17. Dizman, N. et al. Association between time-of-day of immune checkpoint blockade administration and outcomes in metastatic renal cell carcinoma. *Clin. Genitourin. Cancer* **21**, 530–536 (2023).
18. Landré, T. et al. Effect of immunotherapy-infusion time of day on survival of patients with advanced cancers: a study-level meta-analysis. *ESMO Open* **9**, 102220 (2024).
19. Karaboué, A. et al. Why does circadian timing of administration matter for immune checkpoint inhibitors' efficacy? *Br. J. Cancer* **131**, 783–796 (2024).
20. Cortellini, A. et al. A multicentre study of pembrolizumab time-of-day infusion patterns and clinical outcomes in non-small-cell lung cancer: too soon to promote morning infusions. *Ann. Oncol.* **33**, 1202–1204 (2022).
21. Rousseau, A. et al. Clinical outcomes by infusion timing of immune checkpoint inhibitors in patients with advanced non-small cell lung cancer. *Eur. J. Cancer* **182**, 107–114 (2023).
22. Goss, G. et al. LBA48 CTG BR.31: a global, double-blind placebo-controlled, randomized phase III study of adjuvant durvalumab in completely resected non-small cell lung cancer (NSCLC). *Ann. Oncol.* **35**, S1238 (2024).
23. Felip, E. et al. Adjuvant atezolizumab after adjuvant chemotherapy in resected stage IB–IIIA non-small-cell lung cancer (IMpower010): a randomised, multicentre, open-label, phase 3 trial. *Lancet* **398**, 1344–1357 (2021).
24. O'Brien, M. et al. Pembrolizumab versus placebo as adjuvant therapy for completely resected stage IB–IIIA non-small-cell lung cancer (PEARLS/KEYNOTE-091): an interim analysis of a randomised, triple-blind, phase 3 trial. *Lancet Oncol.* **23**, 1274–1286 (2022).
25. Huang, Z. et al. Overall survival according to time-of-day of combined immuno-chemotherapy for advanced non-small cell lung cancer: a bicentric bicontinental study. *EBioMedicine* **113**, 105607 (2025).
26. Miao, K. et al. Peripheral blood lymphocyte subsets predict the efficacy of immune checkpoint inhibitors in non-small cell lung cancer. *Front. Immunol.* **13**, 912180 (2022).
27. Wang, Y., Zhu, J., Zhou, N., Wang, Y. & Zhang, X. Changes in T lymphocyte subsets predict the efficacy of atezolizumab in advanced non-small cell lung cancer: a retrospective study. *J. Thorac. Dis.* **15**, 5669–5679 (2023).
28. Yost, K. E. et al. Clonal replacement of tumor-specific T cells following PD-1 blockade. *Nat. Med.* **25**, 1251–1259 (2019).
29. Zhang, J. et al. Compartmental analysis of T-cell clonal dynamics as a function of pathologic response to neoadjuvant PD-1 blockade in resectable non-small cell lung cancer. *Clin. Cancer Res.* **26**, 1327–1337 (2020).
30. Marcos Rubio, A., Everaert, C., Van Damme, E., De Preter, K. & Vermaelen, K. Circulating immune cell dynamics as outcome predictors for immunotherapy in non-small cell lung cancer. *J. Immunother. Cancer* **11**, e007023 (2023).
31. Spitzer, M. H. et al. Systemic immunity is required for effective cancer immunotherapy. *Cell* **168**, 487–502.e415 (2017).
32. Wang, C. et al. Circadian tumor infiltration and function of CD8⁺ T cells dictate immunotherapy efficacy. *Cell* **187**, 2690–2702 (2024).
33. Fortin, B. M. et al. Circadian control of tumor immunosuppression affects efficacy of immune checkpoint blockade. *Nat. Immunol.* **25**, 1257–1269 (2024).

Publisher's note Springer Nature remains neutral with regard to jurisdictional claims in published maps and institutional affiliations.

Springer Nature or its licensor (e.g. a society or other partner) holds exclusive rights to this article under a publishing agreement with the author(s) or other rightsholder(s); author self-archiving of the accepted manuscript version of this article is solely governed by the terms of such publishing agreement and applicable law.

© The Author(s), under exclusive licence to Springer Nature America, Inc. 2026

Zhe Huang^{1,2,20}, **Liang Zeng**^{1,20}, **Zhaohui Ruan**^{1,3,20}, **Qun Zeng**^{4,20}, **Huan Yan**¹, **Wenjuan Jiang**⁵, **Yi Xiong**⁵, **Chunhua Zhou**⁵, **Haiyan Yang**⁵, **Li Liu**⁵, **Jiacheng Dai**¹, **Nachuan Zou**¹, **Shidong Xu**^{1,2}, **Ya Wang**⁵, **Zhan Wang**⁵, **Jun Deng**¹, **Xue Chen**¹, **Jing Wang**¹, **Hua Xiang**⁶, **Xiaomei Li**⁷, **Boris Duchemann**^{7,8}, **Guoqiang Chen**⁹, **Yang Xia**¹⁰, **Tony Mok**^{11,12} ✉, **Christoph Scheiermann**^{4,13,14,15} ✉, **Francis Lévi**^{17,16} ✉, **Nong Yang**^{5,18} ✉ & **Yongchang Zhang**^{12,5,19} ✉

¹Early Phase Clinical Trial Center, Department of Investigational Cancer Therapeutics, Hunan Cancer Hospital/The Affiliated Cancer Hospital of Xiangya School of Medicine, Central South University, Changsha, China. ²Department of Pathology, School of Basic Medical Science, Central South University, Changsha, China. ³Third Xiangya Hospital, Central South University, Changsha, China. ⁴Department of Pathology and Immunology, Faculty of Medicine, University of Geneva, Geneva, Switzerland. ⁵Department of Medical Oncology, Lung Cancer and Gastrointestinal Unit, Hunan Cancer Hospital/The Affiliated Cancer Hospital of Xiangya School of Medicine, Central South University, Changsha, China. ⁶Department of Interventional Vascular Surgery, Hunan Cancer Hospital/The Affiliated Cancer Hospital of Xiangya School of Medicine, Central South University, Changsha, China. ⁷Research Unit 'Chronotherapy, Cancer, Transplantation', Faculty of Medicine, Paris-Saclay University, Hospital Paul Brousse, Villejuif, France. ⁸Thoracic and Medical Oncology Unit, Avicenne Hospital, Assistance Publique–Hôpitaux de Paris, Bobigny, France. ⁹Key Laboratory of Tropical Translational Medicine of Ministry of Education, School of Basic Medicine, Hainan Academy of Medical Sciences, Hainan Medical University, Haikou, China. ¹⁰Key Laboratory of Respiratory Disease of Zhejiang Province, Department of Respiratory and Critical Care Medicine, Second Affiliated Hospital of Zhejiang University School of Medicine, Hangzhou, China. ¹¹The Chinese University of Hong Kong, Hong Kong, China. ¹²Department of Clinical Oncology, State Key Laboratory of Translational Oncology Hong Kong, Hong Kong, China. ¹³Translational Research Centre in Onco-Hematology (CROH), Geneva, Switzerland. ¹⁴Geneva Center for Inflammation Research (GCIR), Geneva, Switzerland. ¹⁵Biomedical Center (BMC), Institute for Cardiovascular Physiology and Pathophysiology, Walter Brendel Center for Experimental Medicine (WBex), Faculty of Medicine, Ludwig-Maximilians-Universität (LMU) Munich, Planegg-Martinsried, Germany. ¹⁶Gastro-Intestinal and Medical Oncology Department, Paul Brousse Hospital, Assistance Publique–Hôpitaux de Paris, Villejuif, France. ¹⁷Department of Statistics, University of Warwick, Coventry, United Kingdom. ¹⁸Hunan Second People's Hospital, Changsha, China. ¹⁹Furong Laboratory, Changsha, China. ²⁰These authors contributed equally: Zhe Huang, Liang Zeng, Zhaohui Ruan, Qun Zeng. ✉ e-mail: tony@clo.cuhk.edu.hk; christoph.scheiermann@unige.ch; francis.levi@universite-paris-saclay.fr; yangnong0217@163.com; zhangyongchang@csu.edu.cn

Methods

Study design

This prospective, randomized, single-center, open-label phase 3 trial (LungTIME-C01) was designed to compare survival outcomes between patients who received their first four cycles of immunotherapy before 15:00 h and those who received them after 15:00 h. Participants were enrolled at Hunan Cancer Hospital between 22 September 2022 and 21 May 2024.

The trial was registered on ClinicalTrials.gov on 22 September 2022 (NCT05549037, <https://clinicaltrials.gov/search?cond=Lung%20Cancer&term=NCT05549037>) and conducted at Hunan Cancer Hospital. All patients provided written informed consent before enrollment, including consent for publication of de-identified medical data. The full study protocol is provided in the Supplementary Note.

Ethics approval and consent

This study was conducted in accordance with the principles of the Declaration of Helsinki and the guidelines of Good Clinical Practice. The study protocol was reviewed and approved by the Ethics Committee of Hunan Cancer Hospital. All participants provided written informed consent before enrollment.

Patients

Patients aged >18 years with histologically or cytologically confirmed stage III–IV NSCLC, who had not received prior systemic therapy, were enrolled in this trial. In this study, all patients with adenocarcinoma underwent next-generation sequencing (NGS), whereas NGS was not required for patients with squamous cell carcinoma³⁴. Among those who underwent NGS, *EGFR*, *ALK* and *ROS1* sensitizing alterations were all assessed. Patients were excluded if they had symptomatic active central nervous system metastases, a history of pneumonitis requiring glucocorticoid therapy or active autoimmune disease. Complete eligibility criteria are listed in the protocol (see Supplementary Note for full study protocol). All enrolled patients understood the requirements and details of the clinical trial and provided signed informed consent. Patients' biological sex (female/male) was documented, whereas data on sex identity were not recorded. Tumor burden was assessed based on the response evaluation criteria in solid tumors (RECIST) sum of target lesions. The LIPI, defined by a derived neutrophil-to-lymphocyte ratio > 3 and lactate dehydrogenase > upper limit of normal, was used to classify patients into the following three risk groups: low risk (0 factors), medium risk (1 factor) and high risk (2 factors)³⁵.

Study design and treatments

Randomization was performed in a 1:1 ratio using a computer-generated random number table prepared by an independent statistician, without stratification. Due to the nature of infusion scheduling, the study was open-label and blinding of patients and investigators was not feasible. The 15:00 h cutoff time defining early and late ToD treatment groups was determined from a preliminary retrospective analysis of 447 patients at Hunan Cancer Hospital (2017–2021), which identified this time point as yielding the lowest HR for PFS among various candidate cutoff times (see Supplementary Note for full study protocol)²⁵. We exerted strict control on infusion ToD only during the first four cycles^{15,36,37}. Patients in the early ToD group received ICI (pembrolizumab or sintilimab) before 15:00 h, whereas those in the late ToD group received treatment after 15:00 h. Chemotherapy was infused approximately 30 minutes after immunotherapy. After the first four cycles, patients received maintenance therapy with unstipulated infusion times.

Pembrolizumab or sintilimab (200 mg) was given every three weeks until disease progression, death or occurrence of intolerable adverse events. Immunotherapy was combined with chemotherapy every three weeks based on histological type and established guidelines. Patients with squamous cell carcinoma received carboplatin (AUC = 5 mg ml⁻¹ min⁻¹) and nab-paclitaxel (200 mg m⁻²). Patients

with histologically confirmed adenocarcinoma received carboplatin (AUC = 5 mg ml⁻¹ min⁻¹) and pemetrexed (500 mg m⁻²) followed by maintenance pemetrexed after the cycle 4.

PD-L1 immunohistochemistry and scoring

PD-L1 testing was not mandatory in this trial. For patients with available pretreatment tumor tissue, PD-L1 expression was evaluated at our institutional central pathology laboratory. Formalin-fixed paraffin-embedded samples were stained using the 22C3 pharmDx antibody on the Dako Autostainer Link 48 platform, following the manufacturer's instructions and standardized procedures. PD-L1 expression was initially recorded as a continuous TPS (0–100%). For statistical analyses, TPS values were subsequently stratified into conventional categories (<1%, 1–49%, ≥50%). Results were available for 93.33% (196/210) of patients; data for some patients were missing due to insufficient tissue samples. All tissue samples were processed and interpreted using identical procedures in this study, thereby minimizing potential bias.

Endpoints and assessments

The primary endpoint was PFS according to BIRC. Secondary endpoints included OS and objective response rate, also assessed by the BIRC. All the baseline and imaging documents used for response and progressive disease assessments were evaluated by the BIRC, in addition to routine evaluations conducted by the clinical oncology management team. Changes in tumor burden were assessed every two cycles using imaging scans that included computed tomography, magnetic resonance imaging and/or positron emission tomography–computed tomography. All patients underwent brain magnetic resonance imaging with contrast at enrollment. Tumor responses were classified and confirmed according to RECIST criteria (version 1.1)³⁸. Adverse events and laboratory abnormalities were graded according to the National Cancer Institute Common Terminology Criteria for Adverse Events (version 4.0).

Trial oversight

The trial was designed and conducted by an academic group at Hunan Cancer Hospital. The trial protocol, along with all amendments, was approved by the Ethics Committee of Hunan Cancer Hospital. All patients provided written informed consent before enrollment. Biomarker testing was not mandated by the study protocol. Peripheral blood lymphocyte subsets from consenting patients were quantified every two cycles over the initial four cycles. The authors guarantee the accuracy and completeness of the data and the fidelity of the trial to the protocol.

Whole blood lymphocyte subsets analysis

For patients who voluntarily participated in the lymphocyte subset analysis, blood samples were collected between 08:00 h and 10:00 h in the morning at baseline and after cycles 2 and 4 for the quantification of blood cell counts and immune cell subsets. For the volunteering patients who participated in the lymphocyte subset analysis, flow cytometry was performed on the collected samples. The assessed subsets included total T cells (CD3⁺), CD4⁺ T cells (CD3⁺, CD4⁺), CD8⁺ T cells (CD3⁺, CD8⁺), B cells (CD3⁻, CD20⁺) and NK cells (CD16⁺, CD56⁺) (Multitest IMK Kit, BD Biosciences). These subsets were prespecified as exploratory endpoints. The post hoc analysis of activated (CD38⁺HLA-DR⁺CD3⁺CD8⁺) and exhausted (TIM-3⁺PD-1⁺CD3⁺CD8⁺) CD8⁺ T cells was restricted to blood samples with sufficiently well-preserved cells.

Statistical analyses

Sample size calculation was performed using PASS software (version 15.0, NCSS). The log-rank test was applied under the assumption that median PFS was 6 and 10 months in the late and early ToD groups, respectively. The calculation was based on a statistical power of 0.8, a two-tailed significance level of less than 0.05, a group allocation ratio of 1:1 and an anticipated loss to follow-up rate of 5%. Using these parameters, the required sample size was estimated at 210 participants, with 105 per arm.

For continuous variables following a normal distribution, results were presented as mean values with standard deviations or standard error of the mean and compared using Student's *t* test, unless specified otherwise. For non-Gaussian distributed continuous variables, median values, range and interquartile ranges were reported, with comparisons made using the Wilcoxon rank-sum test. Categorical variables were expressed as numbers and percentages, with statistical significance assessed using either the chi-square test or Fisher's exact test. Median follow-up time was estimated using the reverse Kaplan–Meier method, which accounts for censored data and calculates the time point at which 50% of the cohort remained event free. The log-rank test was employed to evaluate between-group differences in OS and PFS. The HRs were estimated using a Cox regression model. Univariate and multivariate Cox regression analyses were also conducted to assess the impact of potential confounding factors on OS and PFS. The proportional hazards assumption for the Cox model was assessed using the Schoenfeld residuals test, implemented via the 'cox.zph' function in the survival package (v3.3.1, <https://github.com/therneau/survival>)³⁹. A *P* value <0.05 was considered indicative of a violation of this assumption.

Comparisons were conducted among patients with complete lymphocyte data at all three time points. Linear regression analyses were used to identify progressive changes in specific lymphocyte subtypes over the course of treatment. The regression line was constrained to start at 1. A repeated two-way analysis of variance was performed to assess the impact of time point and ToD of immunotherapy on the ratios of lymphocyte subsets by using the 'ezANOVA()' function in the ez package (v4.4.0, <https://github.com/mike-lawrence/ez>). The *P* value for the main effect of the ToD group was reported. We compared slopes across ToD groups using the methods presented by Nekola and White. This analysis used the 'diffslope()' function from the simba package (version 0.3-5, <https://cran.r-project.org/web/packages/simba/>)^{40,41}.

Data processing, statistical analyses and figure generation were performed using SPSS (v27.0.1.0; <https://www.ibm.com/spss>), Graph Pad Prism (v9.5.1; <https://www.graphpad.com/>) and R (v4.0.3; <http://www.R-project.org/>).

Reporting summary

Further information on research design is available in the Nature Portfolio Reporting Summary linked to this article.

Data availability

Due to concerns regarding patient privacy and institutional data governance, the clinical datasets generated or used in this study are not publicly accessible. To protect the confidentiality of patients, de-identified individual-level data may be made available upon reasonable request. Researchers interested in accessing the data should contact Y.Z. at Hunan Cancer Hospital. All inquiries will be addressed within approximately 10 weeks. Each request will undergo evaluation by the data oversight committee of Hunan Cancer Hospital to assess compliance with confidentiality policies and potential intellectual property constraints.

References

- Riely, G. J. et al. Non-small cell lung cancer, version 4.2024, NCCN clinical practice guidelines in oncology. *J. Natl. Compr. Canc. Netw.* **22**, 249–274 (2024).
- Kazandjian, D., Gong, Y., Keegan, P., Pazdur, R. & Blumenthal, G. M. Prognostic value of the lung immune prognostic index for patients treated for metastatic non-small cell lung cancer. *JAMA Oncol.* **5**, 1481–1485 (2019).
- Yeung, C., Kartolo, A., Tong, J., Hopman, W. & Baetz, T. Association of circadian timing of initial infusions of immune checkpoint inhibitors with survival in advanced melanoma. *Immunotherapy* **15**, 819–826 (2023).
- Vilalta, A. et al. 967P The time of anti-PD-1 infusion improves survival outcomes by fasting conditions simulation in non-small cell lung cancer. *Ann. Oncol.* **32**, S835 (2021).
- Seymour, L. et al. iRECIST: guidelines for response criteria for use in trials testing immunotherapeutics. *Lancet Oncol.* **18**, e143–e152 (2017).
- Grambsch, P. M. & Therneau, T. M. Proportional hazards tests and diagnostics based on weighted residuals. *Biometrika* **81**, 515–526 (1994).
- Steinitz, O., Heller, J., Tsoar, A., Rotem, D. & Kadmon, R. Predicting regional patterns of similarity in species composition for conservation planning. *Conserv. Biol.* **19**, 1978–1988 (2005).
- Nekola, J. C. & White, P. S. The distance decay of similarity in biogeography and ecology. *J. Biogeogr.* **26**, 867–878 (1999).

Acknowledgements

We are deeply grateful to all the patients and their families who participated in this study. This work received financial support from the National Natural Science Foundation of China (grants 82222048 and 82173338 to Y.Z. and 82003206 to L.Z.). The funding agencies had no role in the study design, data collection, analysis, interpretation, manuscript writing or the decision to submit the article for publication.

Author contributions

Z.H., L.Z., Z.R. conceived the study, collected the data, contributed to the analysis and interpretation of the data, manuscript writing and development of figures and tables. Q.Z. conceived the study, contributed to the analysis and interpretation of the data, manuscript writing and development of figures and tables. H. Yan., W.J., Y. Xiong, C.Z., H. Yang, L.L., J. Dai, N.Z., S.X., Y.W., Z.W., J. Deng and X.C. collected the data, contributed to the analysis and interpretation of the data and to manuscript review and revision. J.W., H.X., X.L., B.D., G.C. and Y. Xia contributed to all collaborative aspects in the study and critically read and improved the manuscript. C.S. conceived the study, contributed to all study progress and development, contributed to methods, results, interpretation and manuscript writing. F.L. conceived the study, contributed to all study progress and development, contributed to methods, results, interpretation and manuscript writing. N.Y. and Y.Z. codirected this study, including conception, organization, data collection, auditing, supervision, project management, funding acquisition, writing and editing the manuscript. T.M. supervised the study and contributed to the writing, review and editing of the manuscript. Z.H., Z.R., L.Z., Q.Z., Y.Z., F.L., C.S. and T.M. verified the underlying data. All authors approved the current manuscript.

Competing interests

The authors declare no competing interests.

Additional information

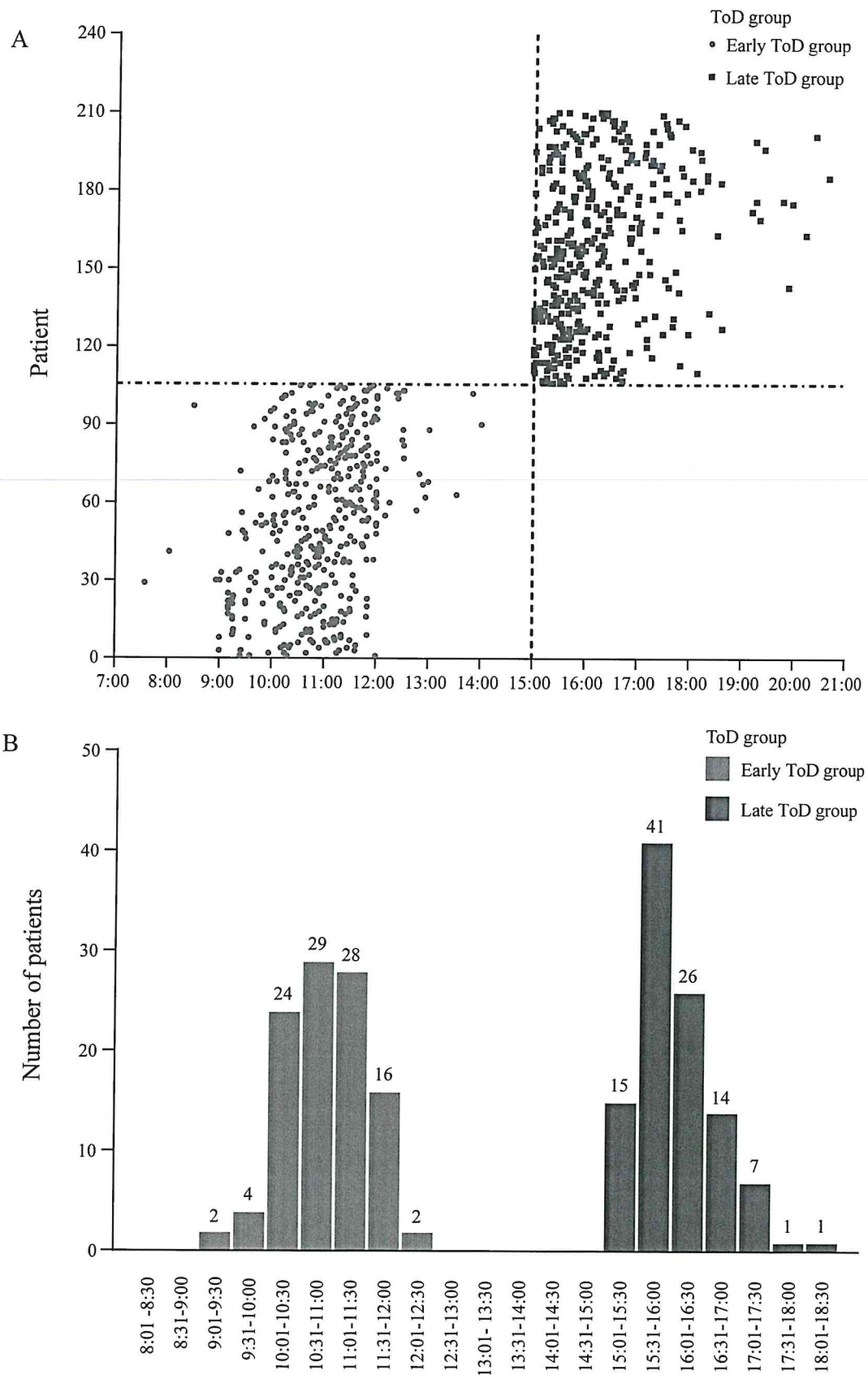
Extended data is available for this paper at <https://doi.org/10.1038/s41591-025-04181-w>.

Supplementary information The online version contains supplementary material available at <https://doi.org/10.1038/s41591-025-04181-w>.

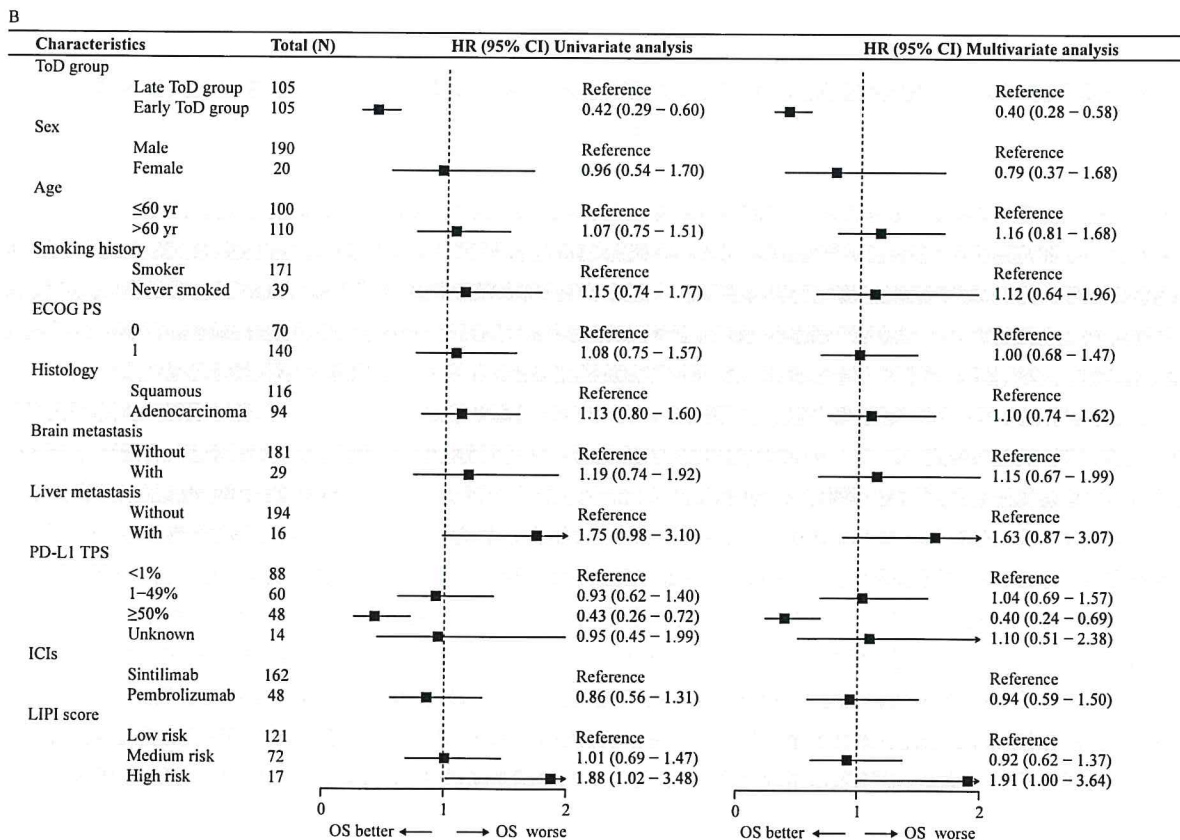
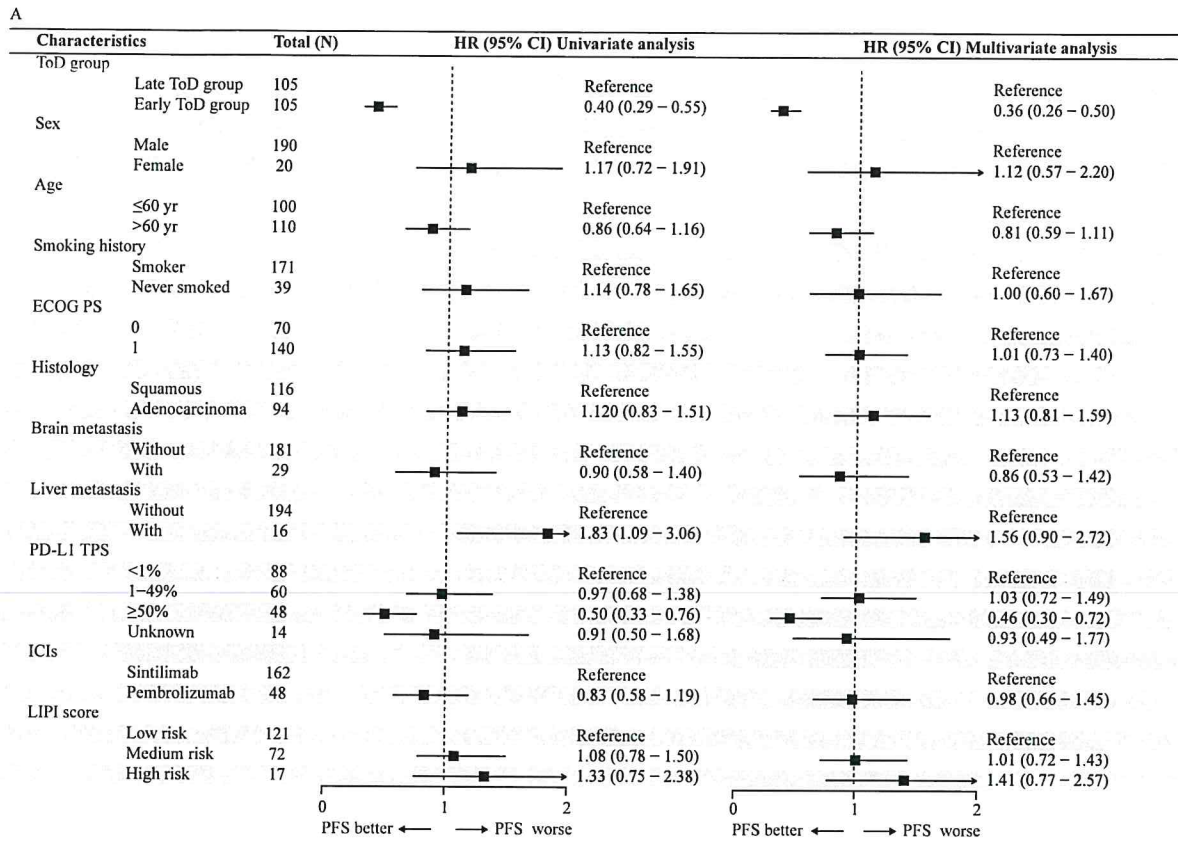
Correspondence and requests for materials should be addressed to Tony Mok, Christoph Scheiermann, Francis Lévi, Nong Yang or Yongchang Zhang.

Peer review information *Nature Medicine* thanks Benjamin Creelan and the other, anonymous, reviewer(s) for their contribution to the peer review of this work. Primary Handling Editor: Ulrike Harjes, in collaboration with the *Nature Medicine* team.

Reprints and permissions information is available at www.nature.com/reprints.



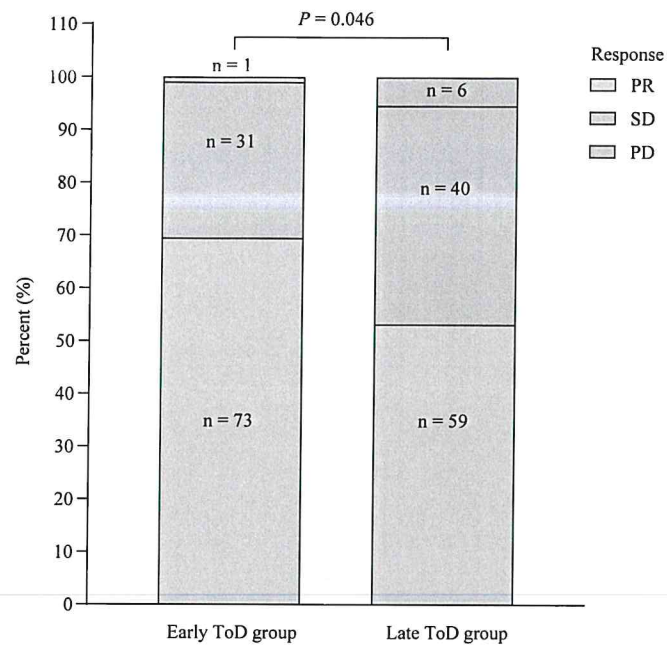
Extended Data Fig. 1 | Distribution of immunotherapy infusion times. (a) Distribution of first 4 infusion times among 210 patients, who were divided into early time-of-day (ToD) infusion group and late ToD group. (b) Histogram of median times of the first 4 infusions per patient (n = 210).



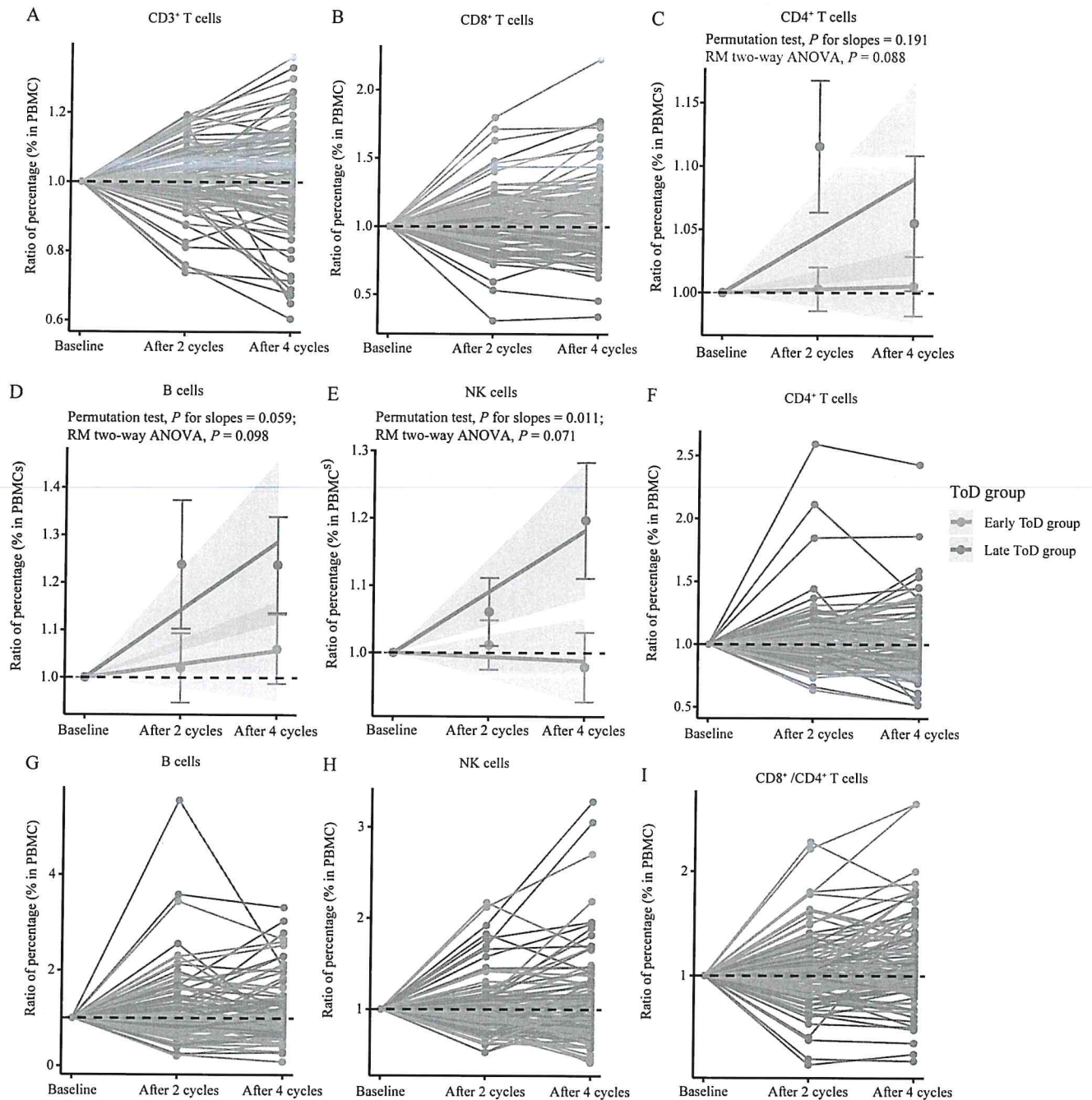
Extended Data Fig. 2 | See next page for caption.

Extended Data Fig. 2 | Univariate and multivariate Cox regression analyses of patient characteristics. (a) Forest plots of the univariate and multivariate Cox regression results for progression-free survival (PFS) (n = 210). (b) Forest plots of the univariate and multivariate Cox regression results for overall survival (OS) (n = 210). P values (two-sided), hazard ratios (HRs), and 95% confidence intervals of HRs were estimated using univariable or multivariable Cox proportional

hazards models, and P values were not adjusted for multiple comparisons. Data are presented as HR (points) with 95% CIs (horizontal lines). ICI, immune checkpoint inhibitor. LUSC, lung squamous cell carcinoma. LUAD, lung adenocarcinoma. ECOG PS, Eastern Cooperative Oncology Group Performance Status. LIPI, Lung Immune Prognostic Index.

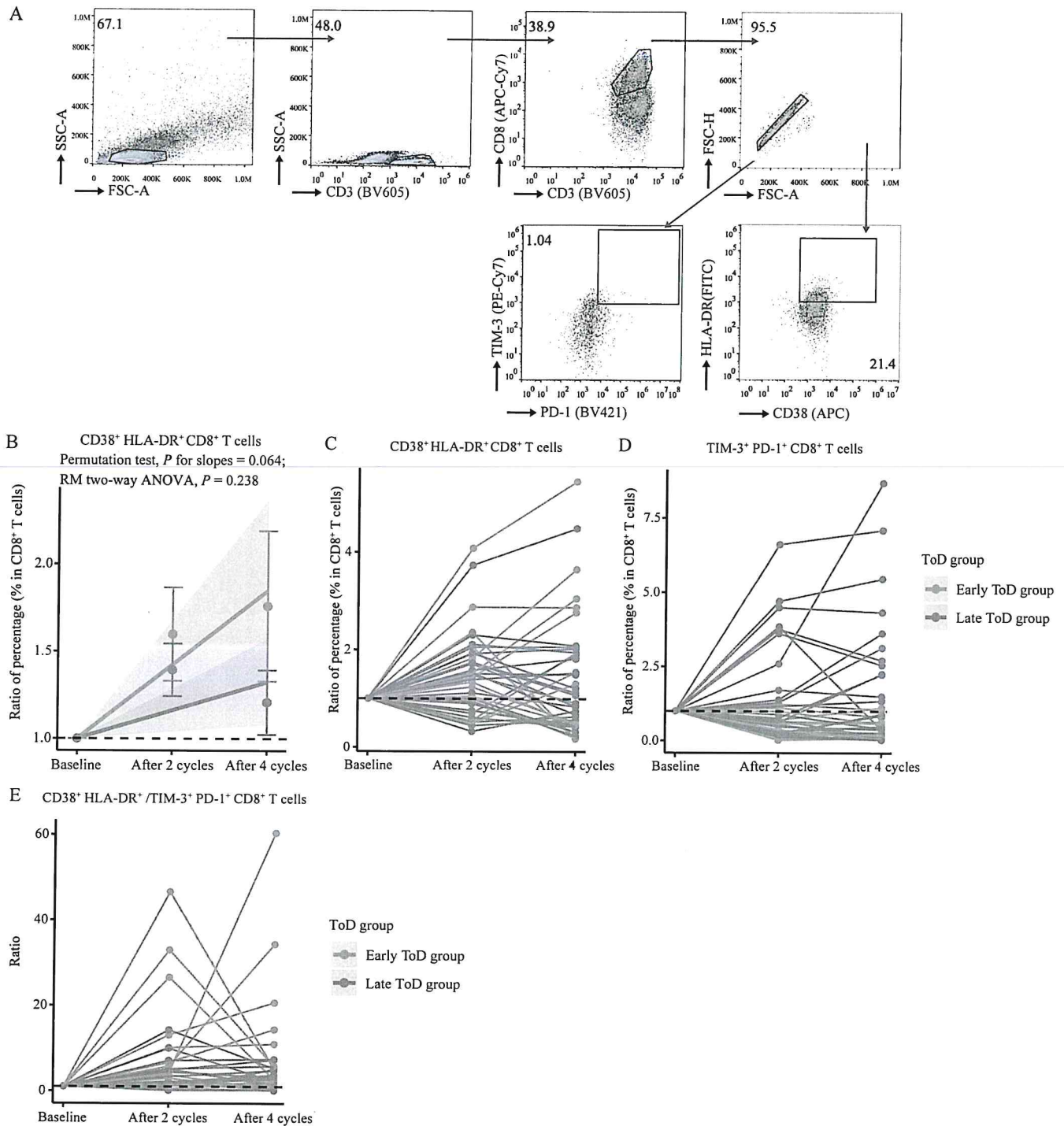


Extended Data Fig. 3 | Response rates of patients according to ToD treatment group. The tumor response was assessed by a blinded independent review committee (BIRC) (n = 210). P values were determined using a two-sided chi-square test. ToD, time-of-day. PR, partial response. SD, stable disease. PD, progressive disease.



Extended Data Fig. 4 | Dynamic alterations of lymphocyte subpopulations in peripheral blood during immunotherapy. Patient values are normalized to individual baseline levels and assessed after 2 cycles (prior to cycle 3) and 4 cycles (prior to cycle 5) of treatment. Line-point graphs depict dynamic changes of CD3⁺ T cell proportion (a), CD8⁺ T cell proportion (b), CD4⁺ T cell proportion (f), B cell proportion (g), NK cell proportion (h) and CD8⁺/CD4⁺ T cell ratio (i) in individual patients from the early and late time-of-day (ToD) groups. Colored lines link sequential measurements from individual patients. The horizontal dotted line represents the normalized baseline (ratio = 1.0). Linear regressions (solid lines) with shaded 95% confidence intervals illustrate changes in CD4⁺ T cell

proportions (c), B cell proportions (d) and NK cell proportions (e) over time in patients from the early and late time-of-day (ToD) groups. Data are presented as mean ± s.e.m. of the mean (s.e.m.). Dotted horizontal lines indicate the normalized baseline (ratio = 1.0). P values were determined using a permutation test (two-sided) and two-way repeated-measures ANOVA (two-sided), without adjustment for multiple comparisons. Flow cytometric analyses of CD4⁺, B and NK cells were performed on paired blood samples collected at baseline, after 2 cycles and after 4 cycles from 61 patients in the early ToD group and 44 patients in the late ToD group (n = 105 total patients; n = 315 total samples).



Extended Data Fig. 5 | Shifts in peripheral lymphocyte subset composition throughout immunochemotherapy administration. Representative flow cytometry gating strategy used to identify CD38⁺ HLA-DR⁺ CD8⁺ T cells and TIM-3⁺ PD-1⁺ CD8⁺ T cells from peripheral blood mononuclear cells (PBMCs) (a). Linear regressions (solid lines) with shaded 95% confidence intervals illustrate changes in CD38⁺ HLA-DR⁺ CD8⁺ T cell proportions (b). Data are presented as mean \pm s.e.m. Dotted horizontal lines indicate the normalized baseline (ratio = 1.0). P values were determined using a permutation test (two-sided) and two-way repeated-measures ANOVA (two-sided), without adjustment for multiple comparisons. Line-point graphs depict dynamic changes of CD38⁺ HLA-DR⁺ CD8⁺ T cell (c), TIM-3⁺ PD-1⁺ CD8⁺ T cell proportion (d) and CD38⁺

HLA-DR⁺ /TIM-3⁺ PD-1⁺ CD8⁺ T cell ratio (e) in individual patients from the early and late time-of-day (ToD) groups. Colored lines connect serial measurements from the same patient. Dotted horizontal lines indicate the normalized baseline (ratio = 1.0). PBMCs, peripheral blood mononuclear cells. Flow cytometric analyses of CD3⁺, CD4⁺, CD8⁺ T, B and NK cells were performed on paired blood samples collected at baseline, after 2 cycles and after 4 cycles from 61 patients in the early ToD group and 44 patients in the late ToD group ($n = 105$ total patients; $n = 315$ total samples). CD38⁺ HLA-DR⁺ CD8⁺ T cells and TIM-3⁺ PD-1⁺ CD8⁺ T cells were assessed in paired cryopreserved PBMCs collected at baseline, after 2 cycles and after 4 cycles from 14 patients in the early ToD group and 25 patients in the late ToD group ($n = 39$ total patients; $n = 117$ total samples).

Extended Data Table 1 | Information about the clinical trial

	Early ToD group	Late ToD group
Enrollment time (year, month)		2022.9 – 2024.5
Duration of follow-up (median)		28.7 months
Duration of treatment (median, IQR)	10.4 (4.9 – 20.5) months	4.5 (2.8 – 8.3) months
No. of chemotherapy-containing cycles (median, range)	4 (1 – 34)	4 (1 – 34)
No. of ICI infusion cycles (median, range)	10 (1 – 40)	6 (1 – 34)
Time of onset of immunochemotherapy during the 4 initial treatment cycles, clock hours (median, range)	10:55 (7:34 – 14:00)	15:57 (15:00 – 20:39)

Extended Data Table 2 | Treatment-related adverse events during all treatments

	Any grade		Grade 3-4	
	Early ToD group (n, %)	Late ToD group (n, %)	Early ToD group (n, %)	Late ToD group (n, %)
Leukopenia	47 (44.8)	30 (28.6)	18 (17.1)	15 (14.2)
Anemia	46 (43.8)	45 (42.9)	16 (15.2)	19 (18.1)
Thrombocytopenia	22 (21.0)	21 (20.0)	8 (7.6)	11 (10.5)
Transaminases increased	9 (8.6)	14 (13.3)	1 (1)	1 (1)
Creatinine increased	7 (6.7)	11 (10.5)	0 (0)	0 (0)
Pruritus	1 (1)	2 (1.9)	0 (0)	1 (1)
Cough	11 (10.5)	15 (14.3)	1 (1)	0 (0)
Hemoptysis	1 (1)	1 (1)	1 (1)	0 (0)
Pneumonia (infectious)	5 (4.8)	6 (5.7)	0 (0)	0 (0)

*Fisher's Exact Test was used to evaluate the association between categorical variables.

Extended Data Table 3 | Immune-related adverse events during all treatments

	Any grade		Grade 3-4	
	Early ToD group (n, %)	Late ToD group (n, %)	Early ToD group (n, %)	Late ToD group (n, %)
Hypothyroidism	12 (11.4)	11 (10.5)	1 (1)	4 (3.8)
Hyperthyroidism	5 (4.8)	4 (3.8)	0 (0)	0 (0)
Rash	13 (12.4)	17 (16.2)	2 (1.9)	2 (1.9)
Pneumonia (immune)	4 (3.8)	5 (4.8)	1 (1)	2 (1.9)
Pancreatitis (immune)	0 (0)	1 (1)	0 (0)	0 (0)
Hepatitis (immune)	1 (1)	1 (1)	0 (0)	1 (1)
Blood glucose increased	4 (3.8)	1 (1)	0 (0)	0 (0)

*Fisher's Exact Test was used to evaluate the association between categorical variables.

Extended Data Table 4 | Baseline demographics and disease characteristics of patients included in the flow cytometry analysis by study group

Characteristics	Early ToD group (n = 61)	Late ToD group (n = 44)	<i>P</i> value
Age			0.284
≤60 yr	30 (49.2)	17 (38.6)	
>60 yr	31 (50.8)	27 (61.4)	
Sex (n, %)			0.758*
Male	54 (88.5)	40 (90.9)	
Female	7 (11.5)	4 (9.1)	
Smoking history (n, %)			0.81
Smoker	51 (83.6)	36 (81.8)	
Never smoked	10 (16.4)	8 (18.2)	
ECOG PS (n, %)			0.889
0	20 (32.8)	15 (31.4)	
1	41 (67.2)	29 (68.6)	
Histology (n, %)			0.809
Squamous	36 (59.0)	21 (61.4)	
Adenocarcinoma	28 (41.0)	23 (38.6)	
Stage (n, %)			0.373
IIIC	14 (23.0)	7 (15.9)	
IV	47 (77.0)	37 (84.1)	
Brain metastasis (n, %)			0.986
Yes	7 (11.5)	6 (11.4)	
No	54 (88.5)	39 (88.6)	
Liver metastasis (n, %)			1.000*
Yes	4 (6.6)	2 (4.5)	
No	57 (93.4)	42 (95.5)	
PD-L1 TPS (n, %)			0.761*
<1%	24 (39.3)	16 (36.4)	
1-49%	16 (26.2)	14 (31.8)	
≥50%	15 (24.6)	12 (27.3)	
Unknown	6 (9.8)	2 (4.5)	
ICIs (n, %)			0.756
Sintilimab	46 (75.4)	32 (72.7)	
Pembrolizumab	15 (24.6)	12 (27.3)	
Tumor burden (n, %)			0.123
≥80 mm	30 (49.2)	15 (34.1)	
<80 mm	31 (50.8)	29 (65.9)	
LDH (n, %)			0.192
≤1 ULN	46 (75.4)	28 (63.6)	
>1 ULN	15 (24.6)	16 (36.4)	
LIPi score (n, %)			0.457*
Low risk	38 (62.3)	24 (54.5)	
Medium risk	18 (29.5)	18 (40.9)	
High risk	5 (8.2)	2 (4.5)	

*Fisher's exact test.

Reporting Summary

Nature Portfolio wishes to improve the reproducibility of the work that we publish. This form provides structure for consistency and transparency in reporting. For further information on Nature Portfolio policies, see our [Editorial Policies](#) and the [Editorial Policy Checklist](#).

Statistics

For all statistical analyses, confirm that the following items are present in the figure legend, table legend, main text, or Methods section.

- | | |
|-----|-----------|
| n/a | Confirmed |
|-----|-----------|
- The exact sample size (n) for each experimental group/condition, given as a discrete number and unit of measurement
 - A statement on whether measurements were taken from distinct samples or whether the same sample was measured repeatedly
 - The statistical test(s) used AND whether they are one- or two-sided
Only common tests should be described solely by name; describe more complex techniques in the Methods section.
 - A description of all covariates tested
 - A description of any assumptions or corrections, such as tests of normality and adjustment for multiple comparisons
 - A full description of the statistical parameters including central tendency (e.g. means) or other basic estimates (e.g. regression coefficient) AND variation (e.g. standard deviation) or associated estimates of uncertainty (e.g. confidence intervals)
 - For null hypothesis testing, the test statistic (e.g. F , t , r) with confidence intervals, effect sizes, degrees of freedom and P value noted
Give P values as exact values whenever suitable.
 - For Bayesian analysis, information on the choice of priors and Markov chain Monte Carlo settings
 - For hierarchical and complex designs, identification of the appropriate level for tests and full reporting of outcomes
 - Estimates of effect sizes (e.g. Cohen's d , Pearson's r), indicating how they were calculated

Our web collection on [statistics for biologists](#) contains articles on many of the points above.

Software and code

Policy information about [availability of computer code](#)

Data collection

Data analysis

For manuscripts utilizing custom algorithms or software that are central to the research but not yet described in published literature, software must be made available to editors and reviewers. We strongly encourage code deposition in a community repository (e.g. GitHub). See the Nature Portfolio [guidelines for submitting code & software](#) for further information.

Data

Policy information about [availability of data](#)

All manuscripts must include a [data availability statement](#). This statement should provide the following information, where applicable:

- Accession codes, unique identifiers, or web links for publicly available datasets
- A description of any restrictions on data availability
- For clinical datasets or third party data, please ensure that the statement adheres to our [policy](#)

To protect patient privacy and comply with institutional data governance policies, the clinical datasets involved in this study are not openly shared. However, de-identified individual-level data can be provided to qualified researchers upon reasonable request. Interested parties may contact Dr. Yongchang Zhang (zhangyongchang@csu.edu.cn) at Hunan Cancer Hospital. All requests will be reviewed by the hospital's data access committee to ensure adherence to privacy regulations and to evaluate potential intellectual property considerations. A formal response will typically be issued within 10 weeks of the inquiry.

Research involving human participants, their data, or biological material

Policy information about studies with [human participants or human data](#). See also policy information about [sex, gender \(identity/presentation\), and sexual orientation](#) and [race, ethnicity and racism](#).

Reporting on sex and gender	We report the sex of patients (biological attribute). The sex classification was based on patient self-reporting and information from family members and confirmed through physician examination.
Reporting on race, ethnicity, or other socially relevant groupings	All participants included in this study were East Asians, having been born and raised in China. Other socially relevant groupings were not considered as variables in this research.
Population characteristics	Of the 210 patients who were randomized, 190 (90.5%) were men and 171 (81.4%) were ever-smokers. PD-L1 tumor proportion scores (TPS) were available in 196 cases (93.3%), with 88 (41.9%) showing TPS <1%, 60 (28.6%) showing TPS 1–49%, and 48 (22.9%) showing TPS ≥50%. Most patients received sintilimab (163, 77.6%), while the remaining 47 (22.4%) were treated with pembrolizumab. Baseline LDH exceeded 1×ULN in 150 patients (72.4%). According to the Lung Immune Prognostic Index, 121 patients (57.6%) were classified as low risk, 72 (34.3%) as intermediate risk, and 12 (8.1%) as high risk.
Recruitment	<p>This study was conducted at Hunan Cancer Hospital. Patient recruitment followed strict inclusion and exclusion criteria as specified in the study protocol.</p> <p>Eligible subjects selected for this study must meet all of the following criteria:</p> <ol style="list-style-type: none"> 1. Understanding the requirements and content of the clinical trial, and providing a signed and dated informed consent form. 2. Male or female patients aged ≥18 years at the time of signing the informed consent form. 3. An Eastern Cooperative Oncology Group (ECOG) performance status of 0-1. 4. Histologically or cytologically confirmed stage IIIC-IV non-small cell lung cancer (NSCLC) with no prior systemic treatment. Disease staging should be based on the 8th edition of the AJCC/UICC NSCLC staging system. 5. Presence of measurable target lesions as defined by RECIST 1.1, confirmed by CT or MRI within 28 days prior to the first dose of study drug. 6. Negative for EGFR, ALK, and ROS1 mutations, as confirmed by a certified laboratory. 7. Patients with stable brain metastases are eligible if no local treatment or steroid tapering is required. 8. FEV1 > 1.0 L and FEV1% > 40%. 9. Adequate hematologic and major organ function defined by the following laboratory criteria, with tests completed within 14 days prior to the first dose of study treatment: <ol style="list-style-type: none"> (1) Hematology (no hematopoietic stimulating factor drugs or blood transfusion within 14 days before the first study treatment): absolute neutrophil count (ANC) ≥ 1.5 × 10⁹/L, absolute lymphocyte count (LC) ≥ 0.5 × 10⁹/L; platelet count (PLT) ≥ 100 × 10⁹/L, hemoglobin (Hb) ≥ 90 g/L (2) Liver function: aspartate transferase (AST) and alanine aminotransferase (ALT) ≤ 3 × ULN; serum total bilirubin (TBIL) ≤ 1.5 × ULN (total bilirubin ≤ 3.0 mg/dL in patients with confirmed Gilbert syndrome); albumin (ALB) ≥ 3 g/dL; (3) Renal function: creatinine clearance rate (CrCl) ≥ 45 mL/minute (by Cockcroft-Gault formula); (4) Coagulation: international normalized ratio (INR) ≤ 1.5, activated partial thromboplastin time (APTT) ≤ 1.5 × ULN; (5) Cardiac color ultrasound: left ventricular ejection fraction (LVEF) ≥ 50% 10. Female or male patients of childbearing potential who are not surgically sterilized must agree to abstain from sexual intercourse (avoid heterosexual intercourse) or use at least one medically acceptable contraceptive (e.g., bilateral tubal ligation, male sterilization, hormonal contraceptives that inhibit ovulation, intrauterine device that releases hormones and copper-containing intrauterine device) during the study treatment period and for 180 days after the end of the study treatment period; female patients of childbearing potential who are not surgically sterilized must have a negative serum HCG test within 14 days before the first dose.
Ethics oversight	This study was performed in compliance with the ethical principles outlined in the Declaration of Helsinki and followed the guidelines of the International Conference on Harmonization for Good Clinical Practice. The protocol received ethical approval from the Hunan Cancer Hospital Institutional Review Board Committee (Expedited Review No. 14 in 2022). Written informed consent was obtained from all participants prior to their inclusion in the study.

Note that full information on the approval of the study protocol must also be provided in the manuscript.

Field-specific reporting

Please select the one below that is the best fit for your research. If you are not sure, read the appropriate sections before making your selection.

- Life sciences Behavioural & social sciences Ecological, evolutionary & environmental sciences

For a reference copy of the document with all sections, see [nature.com/documents/nr-reporting-summary-flat.pdf](https://www.nature.com/documents/nr-reporting-summary-flat.pdf)

Life sciences study design

All studies must disclose on these points even when the disclosure is negative.

Sample size	Sample size calculation was performed using PASS software (version 15.0, NCSS LLC, Kaysville, Utah, USA). The log-rank test module was applied based on the assumption of median PFS at 6 and 10 months in the late and early ToD group, respectively. The calculation was based on a statistical power of 0.8, a two-tailed significance level of less than 0.05, a group allocation ratio of 1:1, and an anticipated loss to follow-up rate of 5%. Using these parameters, the required sample size was determined to be 210 participants, with 105 in each arm.
Data exclusions	No patients were excluded from the data analysis.
Replication	All experimental findings reported in this study are reproducible. Experimental procedures were performed on samples from multiple patients, yielding consistent conclusions. Both statistically significant and non-significant findings are reported.
Randomization	Subjects who meet the study entry criteria will be randomly assigned in a 1:1 ratio to either the Early ToD group or the Late ToD group. Randomization was performed in a 1:1 ratio using a computer-generated random number table prepared by an independent statistician. Group assignments were concealed in sequentially numbered, opaque, sealed envelopes, and were not accessible to study investigators until the point of allocation.
Blinding	Due to the nature of the study, blinding of patients and treating physicians was not feasible, as infusion timing was inherently apparent. Treatment efficacy was assessed by a blinded independent review committee (BIRC).

Reporting for specific materials, systems and methods

We require information from authors about some types of materials, experimental systems and methods used in many studies. Here, indicate whether each material, system or method listed is relevant to your study. If you are not sure if a list item applies to your research, read the appropriate section before selecting a response.

Materials & experimental systems

- n/a Involved in the study
- Antibodies
- Eukaryotic cell lines
- Palaeontology and archaeology
- Animals and other organisms
- Clinical data
- Dual use research of concern
- Plants

Methods

- n/a Involved in the study
- ChIP-seq
- Flow cytometry
- MRI-based neuroimaging

Antibodies

Antibodies used	anti-human PD-1 (CD279) (Thermo Fisher/eBioscience, Cat. no. 62-2799-42, clone eBioJ105 (J105), 5 µL/test), anti-human CD8 (Thermo Fisher/eBioscience, Cat. no. 414-0088-42, clone RPA-T8, 5 µL/test), anti-human TCF-7/TCF-1 (BD Biosciences, Cat. no. 567018, clone S33-966, 5 µL/test), anti-human TIM-3 (CD366) (Thermo Fisher/eBioscience, Cat. no. 12-3109-42, clone F38-2E2, 5 µL/test), anti-human HLA-DR (Thermo Fisher/eBioscience, Cat. no. 45-9956-42, clone LN3, 5 µL/test), anti-human CD3 (Thermo Fisher/eBioscience, Cat. no. 17-0038-42, clone UCHT1, 5 µL/test), anti-human CD38 (Thermo Fisher/eBioscience, Cat. no. 47-0389-42, clone HIT2, 5 µL/test).
Validation	All the antibodies used in this study were commercial antibodies, with validation procedures described on the following sites of the manufacturers: anti-human PD-1 (CD279) (Thermo Fisher/eBioscience, Cat. no. 62-2799-42), https://www.thermofisher.cn/cn/zh/antibody/product/CD279-PD-1-Antibody-clone-eBioJ105-J105-Monoclonal/47-2799-42 anti-human CD8 (Thermo Fisher/eBioscience, Cat. no. 414-0088-42), https://www.thermofisher.cn/cn/zh/antibody/product/CD8a-Antibody-clone-RPA-T8-Monoclonal/414-0088-42 anti-human TCF-7/TCF-1 (BD Biosciences, Cat. no. 567018), https://www.antibodyregistry.org/AB_2916388

anti-human TIM-3 (CD366) (Thermo Fisher/eBioscience, Cat. no. 12-3109-42),
<https://www.thermofisher.cn/cn/zh/antibody/product/CD366-TIM3-Antibody-clone-F38-2E2-Monoclonal/12-3109-42>

anti-human HLA-DR (Thermo Fisher/eBioscience, Cat. no. 45-9956-42),
<https://www.thermofisher.cn/cn/zh/antibody/product/HLA-DR-Antibody-clone-LN3-Monoclonal/45-9956-42>

anti-human CD3 (Thermo Fisher/eBioscience, Cat. no. 17-0038-42),
<https://www.thermofisher.cn/cn/zh/antibody/product/CD3-Antibody-clone-UCHT1-Monoclonal/17-0038-42>

anti-human CD38 (Thermo Fisher/eBioscience, Cat. no. 47-0389-42).
<https://www.thermofisher.cn/cn/zh/antibody/product/CD38-Antibody-clone-HIT2-Monoclonal/47-0389-42>

Clinical data

Policy information about [clinical studies](#)

All manuscripts should comply with the ICMJE [guidelines for publication of clinical research](#) and a completed [CONSORT checklist](#) must be included with all submissions.

Clinical trial registration

Study protocol

Data collection

Outcomes

Plants

Seed stocks

Novel plant genotypes

Authentication

Flow Cytometry

Plots

Confirm that:

- The axis labels state the marker and fluorochrome used (e.g. CD4-FITC).
- The axis scales are clearly visible. Include numbers along axes only for bottom left plot of group (a 'group' is an analysis of identical markers).
- All plots are contour plots with outliers or pseudocolor plots.
- A numerical value for number of cells or percentage (with statistics) is provided.

Methodology

Sample preparation

	<p>gradient centrifugation to isolate peripheral blood mononuclear cells (PBMCs). Flow cytometry was then performed on freshly isolated cells. Remaining cells were resuspended in cryopreservation medium and stored at -80°C for future analysis.</p>
Instrument	<p>BD FACSMelody™ Cell Sorter (BD Biosciences, New Jersey, USA)</p>
Software	<p>Flowjo V10</p>
Cell population abundance	<p>The abundance of total T cells (CD3+), CD4+ T cells (CD3+ CD4+), CD8+ T cells (CD3+ CD8+), B cells (CD3- CD20+), and NK cells (CD16+ CD56+) CD8+ T cells (CD38+ HLA-DR+ CD3+ CD8+) and exhausted CD8+ T cells (TIM-3+ PD-1+ CD3+ CD8+) was determined.</p>
Gating strategy	<p>Lymphocyte subpopulations were identified based on forward scatter/side scatter (FSC/SSC) and surface marker expression. The gating strategy involved exclusion of doublets and debris, followed by sequential gating for CD3, CD4, CD8, CD20, CD16, CD56, CD38, HLA-DR, PD-1, and TIM-3. Boundaries between positive and negative populations were defined using isotype controls and single-stained samples.</p>

Tick this box to confirm that a figure exemplifying the gating strategy is provided in the Supplementary Information.